Regulation of bile acid biosynthesis by hepatocyte nuclear factor 4α

Yusuke Inoue,[*] Ai-Ming Yu,[*] Sun Hee Yim,[*] Xiaochao Ma,[*] Kristopher W. Krausz,[*] Junko Inoue,[*] Charlie C. Xiang,[†] Michael J. Brownstein,[†] Gösta Eggertsen,[§] Ingemar Björkhem,[§] and Frank J. Gonzalez[1,*]

Laboratory of Metabolism, Center for Cancer Research, National Cancer Institute,* and Laboratory of Genetics, National Institute of Mental Health,† National Institutes of Health, Bethesda, MD; and Department of Medical Laboratory Sciences and Technology,§ Huddinge University Hospital, Karolinska Institute, Stockholm, Sweden

Abstract **Hepatocyte nuclear factor 4α (HNF4α) regulates many genes that are preferentially expressed in liver. Mice lacking hepatic expression of HNF4α (HNF4α$^{\Delta L}$) exhibited markedly increased levels of serum bile acids (BAs) compared with HNF4α-floxed (HNF4α$^{F/F}$) mice. The expression of genes involved in the hydroxylation and side chain β-oxidation of cholesterol, including oxysterol 7α-hydroxylase, sterol 12α-hydroxylase (CYP8B1), and sterol carrier protein x, was markedly decreased in HNF4α$^{\Delta L}$ mice. Cholesterol 7α-hydroxylase mRNA and protein were diminished only during the dark cycle in HNF4α$^{\Delta L}$ mice, whereas expression in the light cycle was not different between HNF4α$^{\Delta L}$ and HNF4α$^{F/F}$ mice. Because CYP8B1 expression was reduced in HNF4α$^{\Delta L}$ mice, it was studied in more detail. In agreement with the mRNA levels, CYP8B1 enzyme activity was absent in HNF4α$^{\Delta L}$ mice. An HNF4α binding site was found in the mouse *Cyp8b1* promoter that was able to direct HNF4α-dependent transcription. Surprisingly, cholic acid-derived BAs, produced as a result of CYP8B1 activity, were still observed in the serum and gallbladder of these mice. These studies reveal that HNF4α plays a central role in BA homeostasis by regulation of genes involved in BA biosynthesis, including hydroxylation and side chain β-oxidation of cholesterol in vivo.—** Inoue, Y., A-M. Yu, S. H. Yim, X. Ma, K. W. Krausz, J. Inoue, C. C. Xiang, M. J. Brownstein, G. Eggertsen, I. Björkhem, and F. J. Gonzalez. **Regulation of bile acid biosynthesis by hepatocyte nuclear factor 4α. *J. Lipid Res.* 2006.** 47: **215–227.**

Supplementary key words conditional knockout mice • sterol 12α-hydroxylase • oxysterol 7α-hydroxylase • sterol carrier protein x • cholic acid

Hepatocyte nuclear factor 4α (HNF4α; NR2A1), an orphan member of the nuclear receptor superfamily, regulates many genes that are preferentially expressed in the liver. HNF4α target genes include several serum proteins such as apolipoproteins, blood coagulation factors, cytochromes P450, and enzymes involved in glucose, ammonia, lipid, steroid, and fatty acid metabolism (1, 2). HNF4α is also involved in human genetic diseases; mutations in the HNF4α gene cause maturity-onset diabetes of the young 1 (3), and mutations in HNF4α binding sites were found in the promoter regions of the genes encoding blood coagulation factor IX and HNF1α, causing hemophilia B Lyden and maturity-onset diabetes of the young-3, respectively (4–6).

Targeted disruption of the HNF4α gene was found to be embryo-lethal (7), indicating that HNF4α is an essential factor for mammalian development. To circumvent the problem of embryonic lethality, liver-specific HNF4α-null mice, designated HNF4α$^{\Delta L}$, were produced using the Cre-loxP system (8). These mice exhibited impaired lipid homeostasis and increased serum ammonia levels as a result of decreased expression of hepatic ornithine transcarbamylase (8, 9). In addition, HNF4α$^{\Delta L}$ mice have increased bile acids (BAs), which could have a role in the high

Manuscript received 29 September 2005 and in revised form 26 October 2005.

Published, JLR Papers in Press, November 1, 2005.
DOI 10.1194/jlr.M500430-JLR200

Abbreviations: ACOX2, trihydroxycoprostancyl-coenzyme A oxidase 2; BA, bile acid; CA, cholic acid; CDCA, chenodeoxycholic acid; CPF, cholesterol 7α-hydroxylase promoter factor; CYP7A1, cholesterol 7α-hydroxylase promoter factor; CYP7B1, oxysterol 7α-hydroxylase; CYP8B1, sterol 12α-hydroxylase; CYP27A1, sterol 27-hydroxylase; CYP39A1, oxysterol 7α-hydroxylase; DBP, albumin D site-binding protein; DCA, deoxycholic acid; D-PBE, D-type peroxisomal bifunctional enzyme; DR1, direct repeat 1; FXR, farnesoid X receptor; HNF4α, hepatocyte nuclear factor 4α; HNF4α$^{\Delta L}$, liver-specific hepatocyte nuclear factor 4α-null; HNF4α$^{F/F}$, hepatocyte nuclear factor 4α-floxed; LC-MS/MS, liquid chromatography tandem mass spectrometry; LRH-1, liver receptor homologue-1; MCA, muricholic acid; NTCP, sodium taurocholate cotransporter polypeptide; OATP1, organic anion transporter polypeptide 1; PPARα, peroxisome proliferator-activated receptor α; PXR, pregnane X receptor; RXRα, retinoid X receptor α; SCPx, sterol carrier protein x; SCP2, sterol carrier protein 2; SHP, small heterodimer partner; UDCA, ursodeoxycholic acid; VLACSR, very long chain acyl-coenzyme A synthase-related gene.

[1] To whom correspondence should be addressed.
e-mail: fjgonz@helix.nih.gov

mortality of these mice as they age (8). BAs derived from cholesterol are preferentially produced in the liver, and the resulting BA pool is maintained by enterohepatic circulation. BAs secreted from liver form micelles with hydrophobic compounds, including fatty acids, sterols, and vitamins, and are absorbed from the jejunum and ileum and recycled via the portal venous system. As a result, only a small portion of BA is excreted into urine and feces, and the constant BA pool is maintained by newly synthesized BAs (10). HNF4α$^{\Delta L}$ mice exhibited greatly increased serum BA levels and reduced expression of BA transporters, such as sodium taurocholate cotransporter polypeptide (NTCP) and organic anion transporter polypeptide 1 (OATP1) (8). Furthermore, increased levels of unconjugated and glycine-conjugated BAs in gallbladder were observed in HNF4α$^{\Delta L}$ mice, which were associated with the reduced expression of the very long chain acyl-CoA synthase-related gene (VLACSR) and BA CoA:amino acid *N*-acyltransferase involved in BA conjugation (11). These results indicate that HNF4α plays an important role in the regulation of enterohepatic circulation of BA. BA production is attributable mainly to the neutral and acidic pathways of BA biosynthesis via a cascade of enzymatic reactions (12, 13). Hydroxylation of the steroid nucleus and side chain of cholesterol is catalyzed by enzymes such as cholesterol 7α-hydroxylase (CYP7A1), oxysterol 7α-hydroxylase (CYP7B1), sterol 27-hydroxylase (CYP27A1), and sterol 12α-hydroxylase (CYP8B1). The side chain β-oxidations are catalyzed by the enzymes trihydroxycoprostanoyl-CoA oxidase [acyl-coenzyme A oxidase 2 (ACOX2)], D-type peroxisomal bifunctional enzyme (D-PBE), and sterol carrier protein x (SCPx).

Using gene knockout mice and transient transfection analysis, several transcription factors and/or nuclear receptors, such as the farnesoid X receptor (FXR) (14), liver X receptor (15), CYP7A1 promoter transcription factor (CPF) (16), pregnane X receptor (PXR) (17, 18), peroxisome proliferator-activated receptor α (PPARα) (19), small heterodimer protein (SHP) (20, 21), HNF1α and HNF1β (22, 23), and fibroblast growth factor receptor 4 (24), were shown to regulate genes encoding BA biosynthesis enzymes. In this study, the role of hepatic HNF4α in BA biosynthesis was investigated. In vivo and in vitro data revealed that HNF4α is critical in the regulation of BA biosynthesis.

MATERIALS AND METHODS

Animals

HNF4α$^{\Delta L}$ mice were generated as described previously (8). All experiments were performed with 14, 28, and 45-day-old male HNF4α-floxed (HNF4α$^{F/F}$) mice and HNF4α$^{\Delta L}$ mice. Mice were housed in a pathogen-free animal facility under a standard 12 h light/12 h dark cycle with ad libitum water and chow. All experiments with mice were carried out under Association for Assessment and Accreditation of Laboratory Animal Care guidelines with the approval of the National Cancer Institute Animal Care and Use Committee.

Microarray analysis 1

cDNA fragments from selected mouse genes were obtained by PCR from cDNA clones inserted into the plasmid pBluescript II or pUC18. The majority of the cDNA fragments contained ~400 and 1,000 bp. Before spotting, the PCR fragments were dissolved in 50% DMSO solution to a final concentration of 100 ng/μl. Microarrays were spotted on amino-silane-coated glass slides (Corning, London, UK) using the Affymetrix 417™ Arrayer. Each set of PCR fragments was arranged in six grids. mRNA was prepared from total liver RNA of 45-day-old mice at 10 AM using magnetic beads (Dynal Biotech, Oslo, Norway), and 1–2 μg was subjected to reverse transcription and labeled with the fluorescent dye Cy3 (CyScribe First-Strand cDNA Labeling Kit; Amersham Pharmacia Biotech, Uppsala, Sweden). Prehybridization and hybridization of the slides were carried out in hybridization cassettes at 65°C essentially as described in the Amersham Pharmacia Biosciences manual. The slides were then analyzed with a ScanArray 4000XL (Perkin-Elmer, Foster City, CA).

Microarray analysis 2

Twenty micrograms of pooled total liver RNA from 45-day-old mice (n = 5 for each group) at 10 AM was reverse-transcribed using oligo(dT) primers with either Cy5 or Cy3 dye using the indirect labeling method (25). The raw data were obtained using a GenPix 4000A scanner (Axon, Union City, CA) and further analyzed with National Cancer Institute microarray analysis tools (http://nciarray.nci.nih.gov) for normalization of each individual array. Each experiment was replicated by reciprocally labeling with either Cy3 or Cy5. Final values for differentially expressed genes were obtained from average regression ratios of Cy5/Cy3 (HNF4α$^{\Delta L}$/HNF4α$^{F/F}$) and the reverse value of Cy5/Cy3 (HNF4α$^{F/F}$/HNF4α$^{\Delta L}$).

Northern blot analysis

Northern blot analysis was carried out as described previously (9). All probes were amplified from a mouse cDNA library using gene-specific primers and cloned into pCR II vector (Invitrogen, Carlsbad, CA). Sequences were verified using the CEQ 2000 Dye Terminator cycle sequencing kit (Beckman Coulter, Fullerton, CA) with a CEQ 2000XL DNA Analysis System (Beckman Coulter).

Real-time PCR

Real-time PCR was performed on an ABI PRISM 7900HT sequence detection system (Applied Biosystems, Foster City, CA). Mouse liver cDNAs encoding CYP7A1, CYP27A1, Oxysterol 7α-hydroxylase (CYP39A1), ACOX2, D-PBE, and control 18S RNA were amplified using SYBR Green PCR Master Mix (Applied Biosystems) and 0.3 μM specific oligonucleotide primers (CYP7A1, 5′-GCTGTGGTAGTGAGCTGTTGCA-3′ and 5′-CACAGCCCAGGTATGGAATCA-3′; CYP27A1, 5′-CTGCACTTCCTGCTGACCAAT-3′ and 5′-TGTCAGTGTGTTGGATGTCGTG-3′; CYP39A1, 5′-CTCTTGCAGGCCATATTGGAA-3′ and 5′-ATAGGAGGAGCATTGGCCAGA-3′; ACOX2, 5′-ATGCAAAGCTGGAAACCCAAG-3′ and 5′-CCACCCCGTGCTTTAAATTCTT-3′; D-PBE, 5′-AGCTGTGAGGAAAATGGTGGC-3′ and 5′-TGATTCCGCTTTCTGACGATG-3′; 18S, 5′-AACTTTCGATGGTAGTCGCCG-3′ and 5′-CCTTGGATGTGGTAGCCGTTT-3′). The conditions were 95°C for 10 min followed by 40 cycles of 15 s at 95°C and 1 min at 60°C. The levels of each mRNA are expressed relative to 18S RNA.

Analysis of oxysterols in serum

The serum levels of the oxysterols 7α-, 25-, and 27-hydroxycholestrol were determined by isotope dilution mass spectrometry and the use of deuterium-labeled internal standards as described previously (26).

Total BA analysis

Mice were anesthetized with 2.5% avertin and decapitated, and the trunk blood was collected in a serum separator tube (Becton Dickinson, Franklin Lakes, NJ). The serum was separated by centrifugation at 7,000 *g* for 5 min and stored at −20°C before analysis. The total BA pool was determined as described previously (24). Urine samples and gallbladder biles were diluted 10 times with water and 1,000 times with 10% methanol, respectively, before analysis. The BA content of all samples was measured by colorimetric analysis using a BA analysis kit (Sigma, St. Louis, MO).

Analysis of gallbladder bile

Bile was hydrolyzed and analyzed by GC-MS essentially as described (27) using a Hewlett-Packard 5973 mass-specific detection instrument equipped with a 0.33 μm phase HP-ultra 1 column. The samples were methylated with diazomethane and trimethylsilylated before analysis. The samples were first analyzed by repetitive scanning to identify different BAs. Cholic acid (CA), chenodeoxycholic acid (CDCA), deoxycholic acid (DCA), and ursodeoxycholic acid (UDCA) were quantified by isotope dilution mass spectrometry with the use of deuterium-labeled internal standards and selected ion monitoring. Other BAs were quantified from the chromatogram/total ion current obtained in the analysis of material to which no internal standard had been added. The peak of trihydroxy BAs was compared with that of CA. The peak areas of the dihydroxy BAs were compared with that of DCA.

Analysis of serum BAs

Twenty microliters of a 50 μM dehydrocholic acid solution (in methanol, used as an internal standard) was added to 60 μl of the serum sample. The mixture was deproteinized by the addition of 200 μl of acetonitrile. The sample was vortexed for 10 s and centrifuged at 14,000 *g* at 4°C for 5 min. The supernatant was transferred to a new glass tube and extracted with 2 ml of a mixture of ethyl acetate and *t*-butyl methyl ether (2:1, v/v). After centrifugation at 3,000 *g* at 4°C for 15 min, the organic phase was transferred to a new glass tube and evaporated under a stream of nitrogen gas. The residue was reconstituted in 60 μl of 50% methanol solution containing 0.2% formic acid. Ten microliters of each reconstituted sample was injected for liquid chromatography tandem mass spectrometry (LC-MS/MS) analysis.

Identification and quantitation of intact free BAs by LC-MS/MS

LC-MS/MS analysis was performed on a PE SCIEX API2000 ESI triple-quadrupole mass spectrometer (Perkin-Elmer) controlled by Analyst software. A Phenomenex Luna C18 3 μm, 100 mm × 2 mm inner diameter column (Torrance, CA) was used to separate free BAs. The flow rate through the column at ambient temperature was 0.2 ml/min, and optimal resolution was achieved by elution with a linear gradient of water containing 0.1% formic acid (45%→0%) and methanol (55%→100%) in 10 min at room temperature. The mass spectrometer was operated in the turbo ion spray mode with positive ion detection. The turbo ion spray temperature was maintained at 350°C, and a voltage of 4.8 kV was applied to the sprayer needle. Nitrogen was used as the turbo ion spray and nebulizing gas. The detection and quantification of free and conjugated BAs and the internal standard were accomplished by multiple reaction monitoring with the transition *m/z* 403.3/367.4 for dehydrocholic acid, 359.1/135.0 for lithocholic acid, 375.1/357.2 for free DCA, CDCA, hyodeoxycholic acid, UDCA, and murideoxycholic acid, 373.1/355.3 for free CA, hyocholic acid, and α- and ω-muricholic acid (MCA), and 391.1/355.2 for β-MCA. All raw data were processed using Analyst software. Calibration curves were linear for free DCA, CDCA, hyodeoxycholic acid, UDCA, and murideoxycholic acid concentrations ranging from 0.05 to 10 μM and for free CA, hyocholic acid, and α-, β-, and ω-MCA concentrations ranging from 0.2 to 20 μM.

Western blot analysis

Frozen livers were homogenized in a lysis buffer (9 M urea, 2% Triton X-100, 70 mM dithiothreitol, 10 μg/ml aprotinin, 10 g/ml leupeptin, and 1 mM phenylmethylsulfonyl fluoride) and allowed to sit on ice for 30 min. The homogenate was centrifuged at 12,000 *g* for 30 min at 4°C, and the supernatants were used as whole cell lysates. Total protein (100 μg), determined by the Bio-Rad assay, was diluted with 3× Laemmli sample buffer, incubated at 65°C for 15 min, fractionated by 10% SDS-PAGE, and blotted onto a polyvinylidene difluoride membrane (Amersham Pharmacia Biotech, Piscataway, NJ). The membrane was incubated for 1 h with PBS containing 0.1% Tween 20, 5% dry milk, 6% glycine, and 3% fetal bovine serum and then for 1 h with a 1:1,000 dilution of primary antibodies against mouse CYP7A1 (a generous gift from Dr. David W. Russell, University of Texas Southwestern Medical Center) and β-actin (Santa Cruz Biotechnology, Santa Cruz, CA). After washing, the membrane was incubated for 1 h with a 1:10,000-diluted horseradish peroxidase-conjugated secondary antibody (Santa Cruz Biotechnology), and the reaction product was visualized using SuperSignal West Pico Chemiluminescent Substrate (Pierce, Rockford, IL).

Determination of CYP8B1 enzyme activity

CYP8B1 enzyme activity was determined by a modification of a previous report (28). 7α-Hydroxy-4-cholestene-3-one (Steraloids, Newport, RI) and 7α,12α-hydroxy-4-cholestene-3-one (a gift from Dr. Mizuho Une, Hiroshima University) were used as the substrate and its metabolite, respectively. Livers from CYP8B1-null and wild-type mice were used as negative and positive controls, respectively (29). Incubation reactions were carried out in 100 mM potassium phosphate (pH 7.4) containing 0.5 mg/ml microsomal protein, 2 mM NADPH, and 100 μM 7α-hydroxy-4-cholestene-3-one at 37°C for 10 min with shaking. The reaction was terminated by the addition of 2 ml of ethyl acetate. 6β-Hydroxytestosterone was used as an internal standard. The reaction mixture described above was centrifuged at 1,200 *g* for 5 min, and the upper layer was collected and dried at 40°C under nitrogen gas. The extracted residue was dissolved in 100 μl of methanol, and 10 μl was injected into an LC-MS/MS system for 7α,12α-hydroxy-4-cholestene-3-one detection. The LC-MS/MS system included a PE SCIEX API2000 ESI triple-quadrupole mass spectrometer (Perkin-Elmer) and a Synergi 4 μm MAX-RP, 50 × 2 mm inner diameter column. The flow rate was 0.2 ml/min with 70% methanol and 30% water containing 0.1% formic acid. The mass spectrometer was operated in the turbo ion spray mode with positive ion detection. The turbo ion spray temperature was maintained at 350°C, and a voltage of 5 kV was applied to the sprayer needle. Nitrogen was used as the turbo ion spray and nebulizing gas. The detection and quantitation of

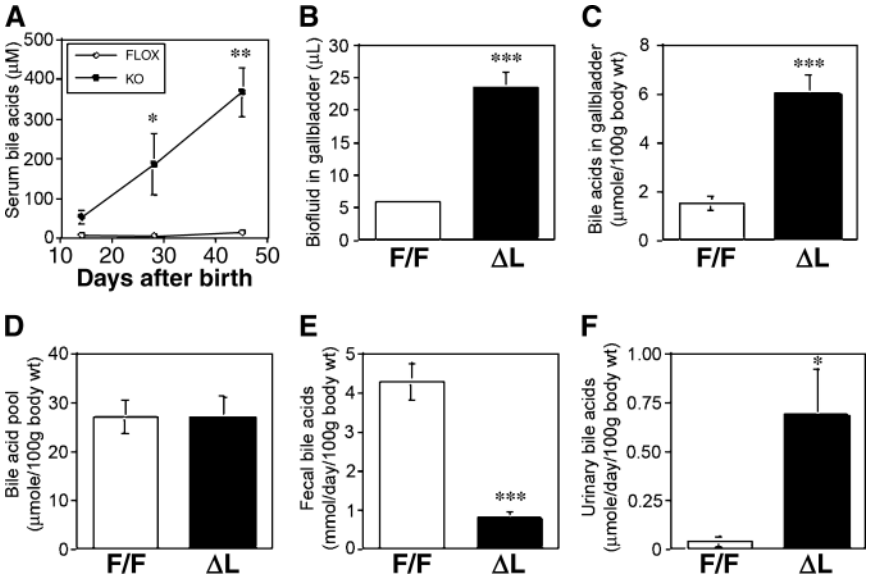

Fig. 1. Bile acid (BA) homeostasis in liver-specific hepatocyte nuclear factor 4α-null (HNF4α$^{\Delta L}$) and hepatocyte nuclear factor 4α-floxed (HNF4α$^{F/F}$) mice. A: Serum total BA levels in 14-, 28-, and 45-day-old mice. B: Total volume of biofluid in gallbladder. C: Total BA amount in gallbladder. D: Total BA pool. E, F: Fecal (E) and urinary (F) BA excretion rates. For B–D, all mice were 45 days old. Data are means ± SEM (HNF4α$^{F/F}$ mice, $n = 4–6$; HNF4α$^{\Delta L}$ mice, $n = 4–8$). Significant differences compared with HNF4α$^{F/F}$ mice: * $P < 0.05$, ** $P < 0.01$, *** $P < 0.001$.

7α,12α-hydroxy-4-cholestene-3-one and 6β-hydroxytestosterone were accomplished by selected ion monitoring with the transition *m/z* 439.1 for 7α,12α-hydroxy-4-cholestene-3-one and 327.2 for 6β-hydroxytestosterone. All raw data were processed using Analyst software. The detection limit for 7α,12α-hydroxy-4-cholestene-3-one is ~0.5 pmol. The sensitivity of the CYP8B1 assay is ~0.1 pmol/min/mg protein.

Construction of the mouse CYP8B1-luciferase reporter plasmids

The −707, −497, −235, −173, and −104/−1 fragments from the translation start site of the mouse *Cyp8b1* promoter (30) containing *Bgl*II and *Kpn*I sites were amplified by PCR and cloned into the luciferase reporter vector, pGL3/basic (Promega, Madison, WI). Mutations were introduced into the putative HNF4α binding site in the *Cyp8b1*-luciferase constructs by PCR-based site-directed mutagenesis using the following complementary primer pair: 5′-ccgagcctctgagcaCTGTCCAAGGGCAggaacct-3′ and 5′-aggttccTGCCCTTGGACAGtgctcagaggctcgg-3′ (Mut; mutations in the HNF4α binding site are underlined). Plasmid DNA sequences were verified with a CEQ 2000XL DNA Analysis System (Beckman Coulter).

Transient transfection assay

HepG2 and CV-1 cell lines were cultured at 37°C in Dulbecco's modified Eagle's medium (Invitrogen) containing 10% fetal bovine serum (HyClone, Logan, UT) and 100 U/ml penicillin/streptomycin (Invitrogen). Cells were seeded on 24-well tissue culture plates and grown to 90–95% confluence. Transfections were carried out as described previously (9). All transfections were performed using Lipofectamine 2000 reagent (Invitrogen) according to the manufacturer's instructions. After 48 h, the cells were washed with phosphate-buffered saline and assayed for dual luciferase activity using commercial kits according to the manufacturer's instructions (Promega).

Gel shift analysis

Crude nuclear extracts were prepared and gel shift analysis was carried out as described previously (9). The following three double-stranded probes were used: HNF4α binding site for the mouse *Cyp8b1* promoter (5′-CTGAGCAAAGTCCAAGGGCAGGAACCT-3′ and 5′-AGGTTCCTGCCCTTGGACTTTGCTCAG-3′), consensus HNF4α binding site, and consensus PPARα response element (Santa Cruz Biotechnology). End-labeled double-stranded oligonucleotide (2×10^5 cpm) was added, and the reaction mixture was incubated at room temperature for 30 min.

TABLE 1. Analysis of free bile acids in serum of HNF4α$^{\Delta L}$ and HNF4α$^{F/F}$ mice

Bile Acid	HNF4α Genotype	
	HNF4α$^{F/F}$	HNF4α$^{\Delta L}$
	μM	
3α,7α,12α-Trihydroxy-5β-cholanoic acid (cholic acid)	0.35 ± 0.18	20.3 ± 2.86[a]
3α,12α-Dihydroxy-5β-cholanoic acid (deoxycholic acid)	0.15 ± 0.04	9.1 ± 2.20[b]
3α,7α-Dihydroxy-5β-cholanoic acid (chenodeoxycholic acid)	0.09 ± 0.03	2.20 ± 0.6[c]
3α,6β,7α-Trihydroxy-5β-cholanoic acid (α-muricholic acid) and 3α,6α,7β-trihydroxy-5β-cholanoic acid (ω-muricholic acid)	0.18 ± 0.05	8.81 ± 1.5[b]
3α,6β,7β-Trihydroxy-5β-cholanoic acid (β-muricholic acid)	0.46 ± 0.27	18.50 ± 3.8[b]
3α,7β-Dihydroxy-5β-cholanoic acid (ursodeoxycholic acid)	0.18 ± 0.07	1.64 ± 0.21[a]

HNF4α, hepatocyte nuclear factor 4α; HNF4α$^{\Delta L}$, liver-specific HNF4α-null; HNF4α$^{F/F}$, HNF4α-floxed. Concentrations and amounts of α- and ω-muricholic acid were combined. Data are means ± SD for 45-day-old HNF4α$^{F/F}$ mice (n = 7–8) and HNF4α$^{\Delta L}$ mice (n = 6–8).

[a] $P < 0.001$ compared with HNF4α$^{F/F}$ mice.

[b] $P < 0.005$ compared with HNF4α$^{F/F}$ mice.

[c] $P < 0.05$ compared with HNF4α$^{F/F}$ mice.

For competition experiments, a 25-fold excess of unlabeled oligonucleotide was added to the reaction mixture and the mixture was incubated at room temperature for 20 min before the addition of a ^{32}P-labeled oligonucleotide probe. For supershift analysis, 1 μg of anti-HNF4α, PPARα, and retinoid X receptor α (RXRα) antibody (Santa Cruz Biotechnology) was added to the reaction mixture, and the mixture was incubated at room temperature for 30 min after the addition of a ^{32}P-labeled oligonucleotide probe.

Statistical analysis

All values are expressed as means ± SEM or SD. All data were analyzed using the unpaired Student's *t*-test for significant differences between the mean values of each group.

RESULTS

Disruption of BA homeostasis in HNF4α$^{\Delta L}$ mice

HNF4α$^{\Delta L}$ mice showed age-dependent increases of serum BA levels; serum BAs in HNF4α$^{\Delta L}$ mice were increased as early as postnatal day 14 and were increased dramatically by 45 days of age compared with those of HNF4α$^{F/F}$ mice (**Fig. 1A**). CA, DCA, CDCA, α-, β-, and ω-MCA, and UDCA were markedly increased, ranging from 10- to 60-fold compared with HNF4α$^{F/F}$ mice, in 45-day-old HNF4α$^{\Delta L}$ mice (**Table 1**). Additionally, a large number of unidentified BAs were also observed in the serum of HNF4α$^{\Delta L}$ mice (data not shown). The expression of

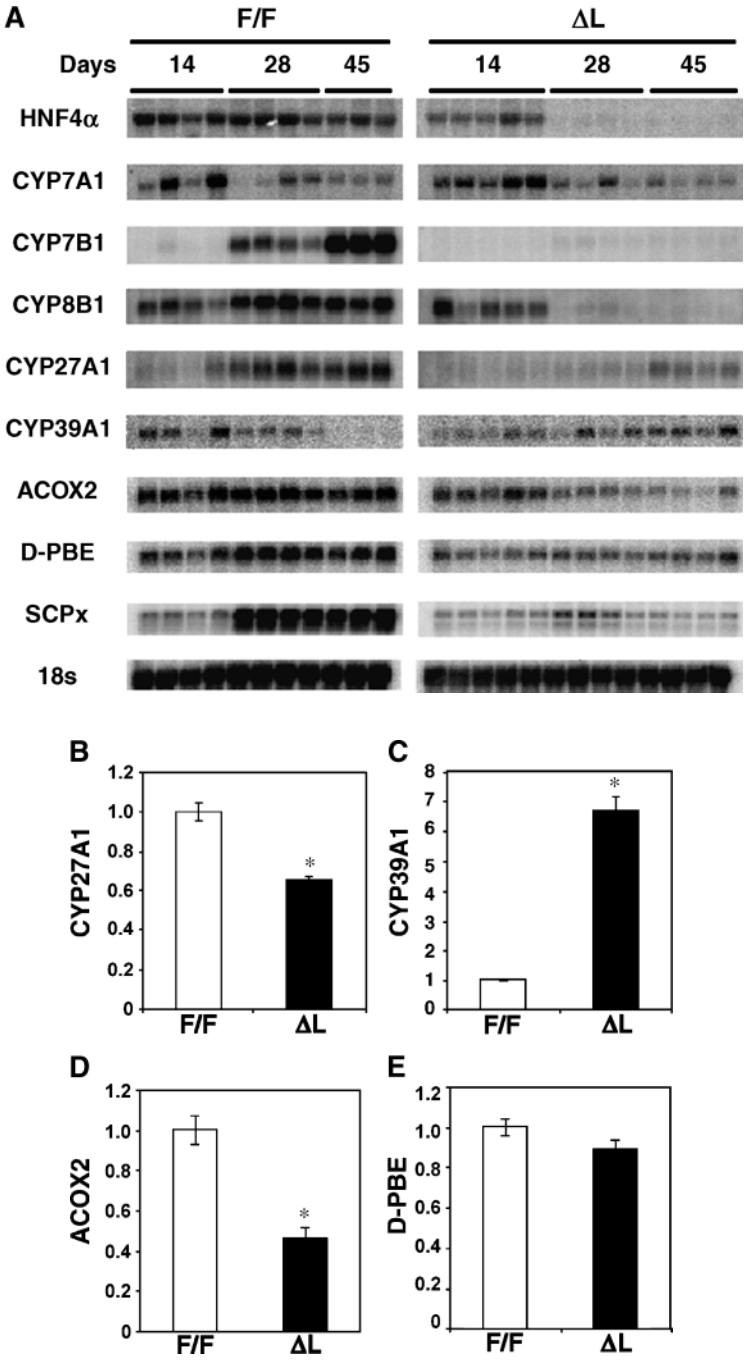

Fig. 2. Expression of the genes involved in BA biosynthesis pathways. A: Northern blot analysis of liver RNA from 14-, 28-, and 45-day-old mice euthanized at 10 AM. B–E: Real-time PCR of liver mRNA from 45-day-old mice euthanized at 10 AM for sterol 27-hydroxylase (CYP27A1; B), CYP39A1 (C), acyl-coenzyme A oxidase 2 (ACOX2; D), and D-type peroxisomal bifunctional enzyme (D-PBE; E). Data are means ± SEM ($n = 8$ for each group). Significant difference compared with HNF4α$^{F/F}$ mice: * $P < 0.001$.

HNF4α was reduced ~50% in the livers of HNF4α$^{\Delta L}$ mice on day 14 and was not detected in 28-day-old HNF4α$^{\Delta L}$ mice (**Fig. 2**), showing that the high serum BA levels in HNF4α$^{\Delta L}$ mice were correlated with the loss of HNF4α expression.

The gallbladders of HNF4α$^{\Delta L}$ mice were much larger than those of HNF4α$^{F/F}$ mice. This was attributable in part to an increase in the volume of biofluid and BA levels in the HNF4α$^{\Delta L}$ mice (Fig. 1B, C). The total BA pool size was similar in both groups (Fig. 1D), whereas the fecal BA excretion rate was decreased (Fig. 1E) and the urinary BA excretion rate was increased (Fig. 1F) in HNF4α$^{\Delta L}$ mice. The total BA excretion rate, derived from the sum of the fecal and urinary BA excretion, was still markedly lower in HNF4α$^{\Delta L}$ mice. BA production in the liver is directly proportional to excreted BA; thus, the synthesis of BA in HNF4α$^{\Delta L}$ mice was decreased compared with that in HNF4α$^{F/F}$ mice.

Expression of genes involved in BA biosynthesis in HNF4α$^{\Delta L}$ mice

To determine the differences in the expression of potential HNF4α target genes involved in BA biosynthesis, microarray analysis was carried out using liver RNA collected from mice killed at 10 AM (**Table 2**). A marked decrease in the expression of genes encoding CYP7B1, CYP8B1, OATP1, and NTCP was found in 45-day-old HNF4α$^{\Delta L}$ mice. Interestingly, there was no significant change in the expression of the *Cyp7a1* gene, whereas expression of the apolipoprotein B gene was decreased and mRNAs encoding HMG-CoA synthase, scavenger receptor class B type I, PXR, RXRα, and LCAT were increased in the HNF4α$^{\Delta L}$ mice. No increased expression of PXR and RXRα mRNAs was observed, as revealed in earlier studies using Northern blot analysis (8). The differentially expressed genes between HNF4α$^{\Delta L}$ and HNF4α$^{F/F}$ mice by microarray analysis were further confirmed by Northern blot analysis and real-time PCR. By Northern analysis, the levels of CYP7A1 mRNA were not significantly different between HNF4α$^{\Delta L}$ and HNF4α$^{F/F}$ mice at the ages tested (Fig. 2A); however, serum levels of 7α-hydroxycholesterol, which reflects the enzymatic activity of CYP7A1 (31), were significantly reduced in HNF4α$^{\Delta L}$ mice (10 ± 1 ng/ml) compared with HNF4α$^{F/F}$ mice (17 ± 1 ng/ml). CYP27A1 and CYP7B1 mRNA levels were reduced significantly in the livers of HNF4α$^{\Delta L}$ mice (Fig. 2A, B). However the serum levels of 27-hydroxycholesterol, the product of CYP27A1 and the substrate for CYP7B1 (32), were >2-fold higher in HNF4α$^{\Delta L}$ mice than in HNF4α$^{F/F}$ mice (118 vs.

TABLE 2. Gene expression changes in HNF4α$^{\Delta L}$ mice-I

Gene Names and Symbols	Regression Ratio
Apolipoprotein A-I	0.87
Apolipoprotein B	0.54
Apolipoprotein E	0.91
Cholesterol 7α-hydroxylase (CYP7A1)	0.82
Oxysterol 7α-hydroxylase (CYP7B1)	0.04
Sterol 12α-hydroxylase (CYP8B1)	0.02
Sterol 27-hydroxylase (CYP27A1)	1.19
3-Hydroxy-3-methylglutaryl CoA synthase (HMG-CoA synthase)	3.24
Sterol regulatory element binding protein-1 (SREBP-1)	1.57
SREBP cleavage-activating protein (SCAP)	1.01
Low density lipoprotein receptor (LDL-R)	1.13
Scavenger receptor class B type I (SR-BI)	2.39
Farnesoid X receptor (FXR)	1.45
Pregnane X receptor (PXR)	2.48
Retinoid X receptor α (RXRα)	2.27
Small heterodimer partner (SHP)	0.61
Lecithin:cholesterol acyltransferase (LCAT)	1.65
Epoxide hydrolase-1 (EH-1)	1.11
Sodium taurocholate cotransporter polypeptide (NTCP)	0.37
Organic anion transporter polypeptide 1 (OATP1)	0.06
Farnesyl diphosphate synthase (FPP synthase)	0.70
ATP binding cassette transporter G5 (ABCG5)	1.51
ATP binding cassette transporter G8 (ABCG8)	0.67
Fatty acid synthase (FAS)	0.66
Tubulin α	0.93
Glyceraldehyde 3-phosphate dehydrogenase (GAPDH)	1.27

Pooled liver total RNA (n = 8 for each genotype) from 45-day-old mice at 10 AM was used. Regression ratio is expressed relative to HNF4α$^{F/F}$ mice.

TABLE 3. Gene expression changes in HNF4α$^{\Delta L}$ mice-II

Gene	GenBank Entry	Regression Ratio
α-2-macroglobulin	NM_175628	0.06
Dolichol-phosphate (β-D) mannosyltransferase 2	NM_010073	0.11
Pleckstrin homology-like domain, family A, member	NM_009344	0.13
Interferon-inducible protein1	NM_008326	0.13
Dihydrofolate reductase	L26316	0.14
18-pending NY-REN-18 antigen	NM_016736	0.14
Promyelocytic leukemia	NM_008884	0.15
Heme binding protein	AB013095	0.17
Vitronectin	M77123	0.17
Apoptosis-antagonizing transcription factor	NM_019816	0.18
Glutaryl-CoA dehydrogenase	U18992	0.18
Annexin A2	NM_007585	0.18
Progesterone receptor membrane component 1	NM_016783	0.18
Transthyretin	NM_013697	0.18
Tight junction protein 1	NM_009386	0.19
Aldehyde dehydrogenase family 1, subfamily A1	NM_013467	0.19
Ras homolog gene family, member C	NM_007484	0.19
Solute carrier family 38, member 3	NM_023805	0.21
WW domain-containing protein 4	NM_153085	0.21
CD9 antigen	NM_007657	0.23
Sterol carrier protein 2	M62361	0.23
Protein phosphatase 2A, catalytic subunit β	Z67746	1.60
Mast cell protease 4	NM_010779	1.82
Prenylated Rab acceptor	AF252856	1.83
Ankyrin repeat hooked to zinc finger motif	NM_009671	1.85
Zinc finger protein 216	NM_009551	1.86
Dynein, cytoplasmic, light chain 1	NM_019682	2.10
Syndecan 2	NM_008304	2.24
Rnp24-pending coated vesicle membrane protein	NM_019770	2.56

Pooled liver total RNA (n = 5 for each genotype) from 45-day-old mice at 10 AM was used. Regression ratio is expressed relative to HNF4α$^{F/F}$ mice.

49 ng/ml). This was also the case with serum levels of 25-hydroxycholesterol (17 vs. 6 ng/ml), a second substrate for CYP7B1 (32, 33). The levels of CYP8B1 mRNA were also markedly reduced in HNF4α$^{\Delta L}$ mice (Fig. 2A). The expression of another CYP7B1 (CYP39A1), with specificity for 24-hydroxycholesterol as a substrate (34), was much higher in adult HNF4α$^{\Delta L}$ mice (Fig. 2A, C).

Expression of mRNAs encoding trihydroxycoprostanoyl-CoA oxidase (ACOX2) and SCPx was also reduced significantly in HNF4α$^{\Delta L}$ mice (Fig. 2A, D), but expression of D-PBE mRNA was unchanged (Fig. 2A, E). Candidate genes were also detected using a cDNA microarray with liver RNA collected at 10 AM (**Table 3**). Decreased expression of mRNA encoding sterol carrier protein 2 (SCP2), which is an alternatively spliced variant of SCPx, and a shorter transcript derived from a different promoter from the SCPx promoter (35) was found. Expression of SCP2 was unchanged using a SCP2-specific probe (data not shown), but SCPx was decreased significantly in HNF4α$^{\Delta L}$ mice using a specific probe that recognizes SCP2 and SCPx (Fig. 2A).

Expression of CYP7A1 is not induced during the dark cycle in HNF4α$^{\Delta L}$ mice

The data in Table 2 and Fig. 2, derived from mice killed in the morning, revealed no difference in CYP7A1 expression between genotypes. However, the expression of CYP7A1 is known to be regulated by circadian rhythm (36, 37). To determine whether the loss of HNF4α affected the response of the gene to light, CYP7A1 mRNA and protein levels were examined (**Fig. 3**). The expression of CYP7A1 mRNA in the livers of HNF4α$^{\Delta L}$ mice was unchanged compared with that of HNF4α$^{F/F}$ mice in the light cycle at 10 AM (Fig. 3A), as revealed by microarray and Northern blot analyses (Fig. 2A). In marked contrast, the expression of CYP7A1 in the dark cycle at 10 PM was increased in HNF4α$^{F/F}$ control mice compared with HNF4α$^{\Delta L}$ mice (Fig. 3B). These results were further confirmed by real-time PCR; CYP7A1 mRNA was not different at 10 AM between HNF4α$^{\Delta L}$ and HNF4α$^{F/F}$ mice but was increased significantly in HNF4α$^{F/F}$ mice but not in HNF4α$^{\Delta L}$ mice at 10 PM (Fig. 3C). Similarly, the expression of CYP7A1 protein was not different between HNF4α$^{F/F}$ and HNF4α$^{\Delta L}$ mice at 10 AM (Fig. 3C) but decreased in HNF4α$^{\Delta L}$ mice compared with HNF4α$^{F/F}$ mice at 10 PM (Fig. 3D). Thus, the increase in the serum levels of 7α-hydroxycholesterol during the light cycle could be attributable to the increased CYP7A1 mRNA found in the HNF4α$^{F/F}$ mice at 10 PM compared with the HNF4α$^{\Delta L}$ mice. In contrast, mRNA encoding CYP8B1 was higher during the light cycle in HNF4α$^{F/F}$ mice but remained low in the HNF4α$^{\Delta L}$ mice (Fig. 3A, B). CYP7B1 and CYP27A1 mRNA levels were not influenced by the light and dark cycles (Fig. 3A, B).

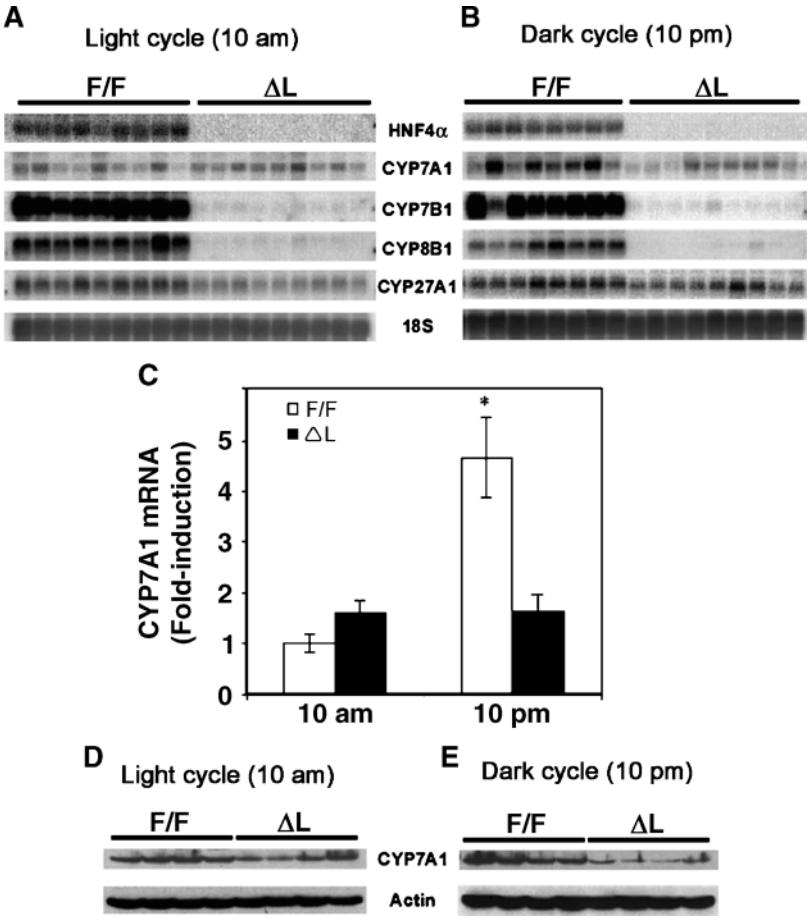

Fig. 3. Circadian rhythm of the expression of cholesterol 7α-hydroxylase (CYP7A1) and sterol 12α-hydroxylase (CYP8B1) mRNAs in the livers of HNF4α$^{\Delta L}$ and HNF4α$^{F/F}$ mice. A, B: Northern blot analysis of mRNA in livers from 45-day-old mice at 10 AM (A) and 10 PM (B). C: Real-time PCR of liver mRNA for CYP7A1 at 10 AM (left) and 10 PM (right). Data are means ± SEM (n = 8 for each group). Significant differences compared with the other three groups: * $P < 0.01$. D, E: Western blots of total liver proteins (100 μg) at 10 AM (D) and 10 PM (E). CYP7A1 and β-actin polyclonal antibodies were used to assess protein expression.

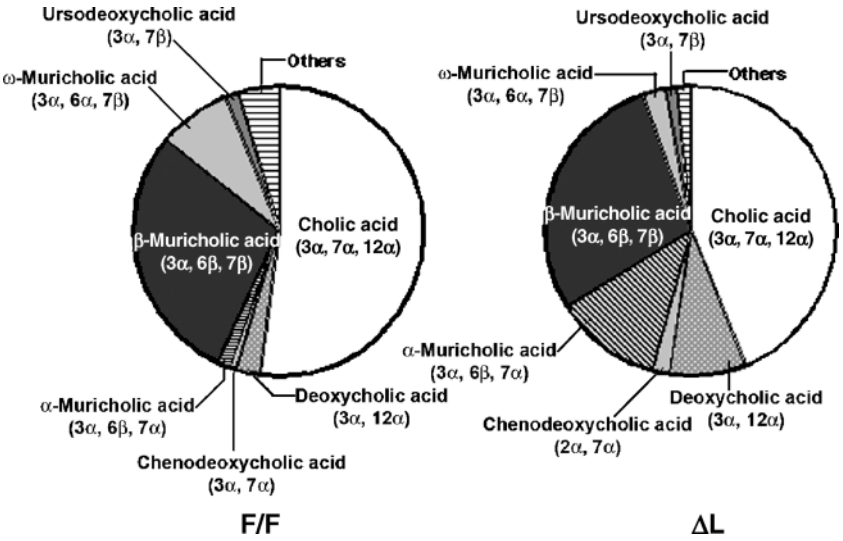

Fig. 4. Composition of BA in HNF4α$^{\Delta L}$ and HNF4α$^{F/F}$ mice. Amounts of individual BAs from 45-day-old mice were analyzed by GC-MS and are indicated as percentages of the entire pool. The position and stereochemistry of hydroxyl groups on the ring structure of each BA are indicated in parentheses.

BA composition in HNF4α$^{\Delta L}$ and HNF4α$^{F/F}$ mice

The expression of several genes encoding enzymes involved in BA biosynthesis was reduced in the livers of HNF4α$^{\Delta L}$ mice, suggesting that the BA composition also might be altered in these mice. In particular, the fact that *Cyp8b1*-null mice lack synthesis of CA (29) suggests that HNF4α$^{\Delta L}$ mice should also be devoid of CA. The composition of gallbladder BA was quantified by GC-MS (**Fig. 4**). In male control HNF4α$^{F/F}$ mice, the primary BAs, CA (52.2%) and β-MCA (29%), accounted for ~82% of the total BAs. The remaining metabolites were DCA (2.7%), α-MCA (1.5%), ω-MCA (8%), CDCA (0.7%), and UDCA (1.8%). On the other hand, CA was decreased to 44%, but its secondary metabolite DCA was increased 3-fold (8.4%), in HNF4α$^{\Delta L}$ mice, indicating that the overall amount of CA-derived metabolites (CA and DCA) was unchanged in HNF4α$^{\Delta L}$ mice (52.4%) versus that in control HNF4α$^{F/F}$ mice (54.9%).

Hepatic CYP8B1 enzyme activity is reduced in HNF4α$^{\Delta L}$ mice

To further investigate the ratio of CA-derived BAs in HNF4α$^{\Delta L}$ mice, the activity of hepatic CYP8B1 was measured. The expression of CYP8B1 is also regulated by circadian rhythm, and the expression pattern during the dark/light cycle is opposite from that of CYP7A1: it is highly expressed during the light cycle and minimally expressed during the dark cycle (36, 37). Northern blot analysis revealed that expression of CYP8B1 in control mice at 10 AM was higher than that at 10 PM (Fig. 3A, B). Furthermore, the expression of CYP8B1 in HNF4α$^{\Delta L}$ mice was reduced markedly in both cycles compared with that in HNF4α$^{F/F}$ mice. CYP8B1 enzyme activity in control mice was also significantly higher at 10 AM than at 10 PM, and the activity in HNF4α$^{\Delta L}$ mice was again reduced markedly at both cycles (**Fig. 5A**). This assay was specific to CYP8B1, because no activity was observed in the livers of *Cyp8b1*-null mice (Fig. 5B).

HNF4α directly binds to the promoter region of the mouse *Cyp8b1* and positively regulates its expression

Because CYP8B1 is expressed mainly in liver (38), the possibility was investigated that HNF4α can directly bind to and regulate the promoter of the mouse *Cyp8b1* gene. The mouse *Cyp8b1* promoter contains a direct repeat 1 (DR1) motif (at position −109 to −94 from the translation start site) that is a potential binding site for nuclear receptors such as HNF4α and PPARα. To determine whether

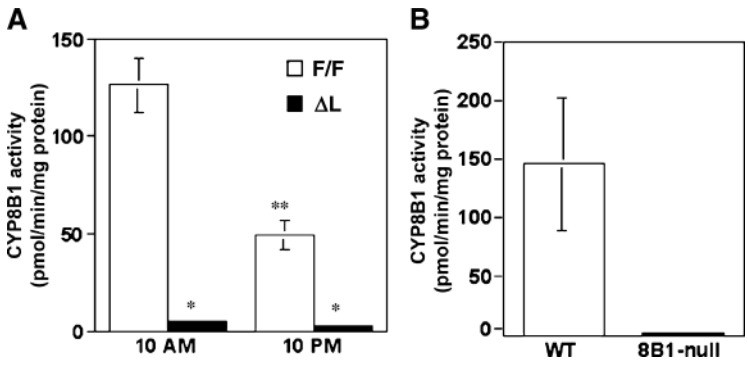

Fig. 5. Specific activities and expression of CYP8B1 in HNF4α$^{\Delta L}$ and HNF4α$^{F/F}$ mice. A: Specific activities of CYP8B1 were measured using liver microsomal protein from HNF4α$^{\Delta L}$ and HNF4α$^{F/F}$ mice. Data are means ± SEM (n = 5). Significant differences between HNF4α$^{\Delta L}$ and HNF4α$^{F/F}$ mice: * $P < 0.001$ and ** $P < 0.005$, respectively. B: Specific activities of CYP8B1 were measured using liver microsomal protein from *Cyp8b1*-null and wild-type (WT) mice. Data are means ± SEM ($n = 2$).

HNF4α is able to activate the mouse *Cyp8b1* promoter, several *Cyp8b1* promoter-luciferase reporter plasmids were constructed (**Fig. 6A**). When the human hepatoma-derived HepG2 cells, which express HNF4α, were used for transient transfections, the promoter activity of the −115 bp fragment containing a putative HNF4α binding site was ~6-fold higher than that of the promoterless construct (pGL3/basic) and the −90 bp fragment (Fig. 6A). The activities of the longer DNA fragments were 6- to 9-fold higher than that of the −115 bp fragment. To determine whether this activity was attributable to HNF4α, CV-1 cells, which do not express HNF4α, were used for the transfection experiments. The promoter activity of the −90 bp fragment was unchanged by cotransfection of the HNF4α expression vector, consistent with the absence of an HNF4α binding site (Fig. 6B). However, the activity of the −115 bp fragment containing the HNF4α binding site was increased by cotransfection with an HNF4α expression vector. Similar results were obtained with the longer DNA fragments; however, the activities with these DNAs were much greater than that of the −115 bp fragment in both CV-1 cells (Fig. 6B) and HepG2 cells (Fig. 6A).

To determine whether HNF4α can bind to the DR1-like element in the mouse *Cyp8b1* promoter, gel shift analysis was performed with ^{32}P-labeled probes (Fig. 6C). Liver

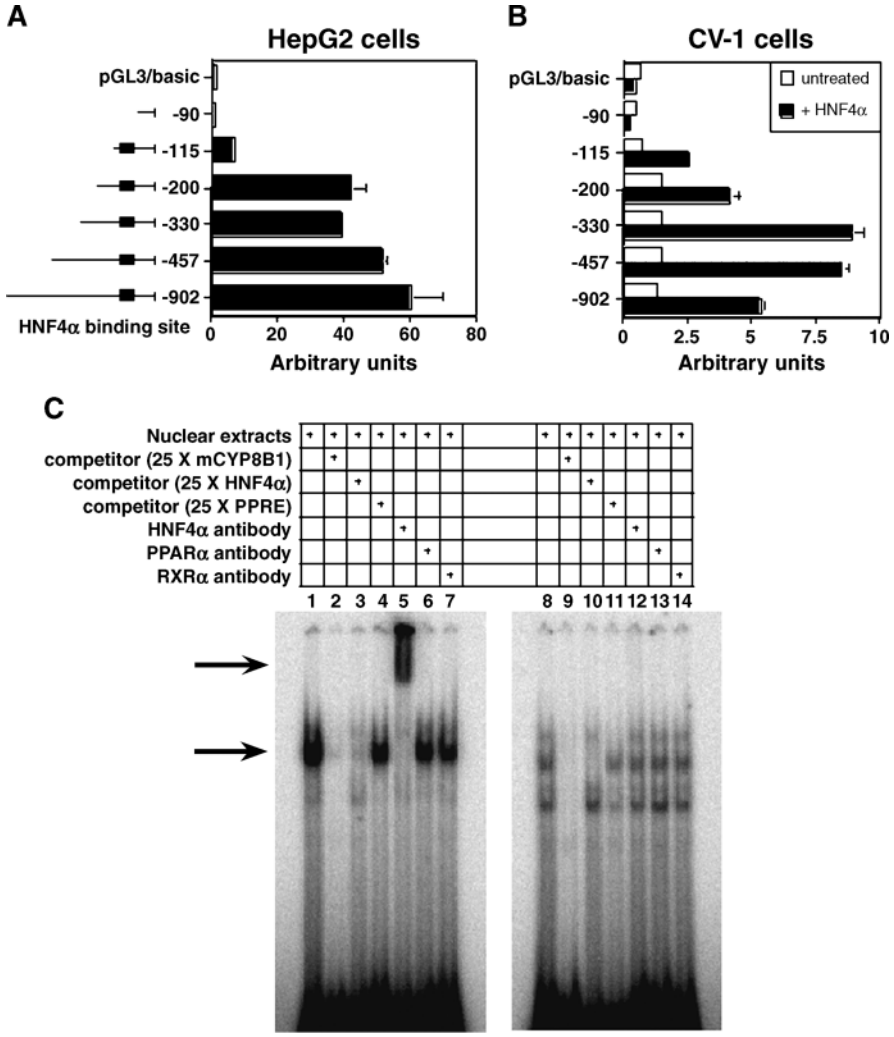

Fig. 6. Promoter analysis of the mouse *Cyp8b1* gene. A: Luciferase reporter plasmids containing the mouse *Cyp8b1* promoter were transfected into HepG2 cells. The normalized activity ± SEM ($n = 4$) of each construct is presented as arbitrary units. B: CV-1 cells were cotransfected with the HNF4α expression vector, as indicated. The normalized activity ± SEM ($n = 4$) of each construct is presented as arbitrary units. C: Nuclear extracts from liver of HNF4α$^{F/F}$ mice (left panel) and HNF4α$^{\Delta L}$ mice (right panel) were incubated with a labeled HNF4α binding site derived from the mouse *Cyp8b1* promoter in the absence (lanes 1 and 8) or presence of each unlabeled oligonucleotide for the HNF4α binding site of the mouse *Cyp8b1* promoter (lanes 2 and 9), consensus HNF4α binding site (lanes 3 and 10), and consensus peroxisome proliferator-activated receptor α (PPARα)-responsive element (lanes 4 and 11). For the supershift assay, nuclear extracts were incubated with labeled oligonucleotide probe in the presence of anti-HNF4α (lanes 5 and 12), anti-PPARα (lanes 6 and 13), and anti-retinoid X receptor α (RXRα) antibodies (lanes 7 and 14). The HNF4α-DNA complex and its supershifted complex, caused by the HNF4α-specific antibody, are indicated by the lower and upper arrows, respectively.

nuclear extracts from HNF4α$^{F/F}$ mice contained proteins that bound to the HNF4α binding site (Fig. 6C, lane 1, lower arrow). The HNF4α-specific binding was diminished by the addition of excess amounts of unlabeled probe and HNF4α consensus sequence but not by a PPARα-responsive element (Fig. 6C, lanes 2–4). Furthermore, these bands were supershifted by the addition of anti-HNF4α antibody, indicating that the protein bound to the DR-1-like element was indeed HNF4α (Fig. 6C, lane 5, upper arrow). The specificity of binding was demonstrated by the lack of a supershift by antibodies against PPARα and RXRα (Fig. 6C, lanes 6, 7). As expected, no HNF4α-specific supershifted bands were detected when liver nuclear extracts from HNF4α$^{\Delta L}$ mice were used (Fig. 6C, lane 12). These results indicate that the DR-1-like element in the mouse *Cyp8b1* promoter has HNF4α-specific binding capacity.

To determine whether disruption of the HNF4α binding site in the *Cyp8b1* gene affects promoter activity, mutations were introduced into the site in the (−330)-luciferase promoter construct (**Fig. 7A**, Mut). As shown in Fig. 7B, when HepG2 cells were used for transient transfections, promoter activity of the mutated −330 bp fragments (−330/Mut) was reduced to background levels compared with that of the wild-type promoter (−330/WT). Similarly, when CV-1 cells were used, the promoter activity of the mutated fragment was not induced by cotransfection of HNF4α expression vector (Fig. 7C). Together, the results shown in Figs. 6 and 7 suggest that HNF4α directly regulates the expression of the *Cyp8b1* gene.

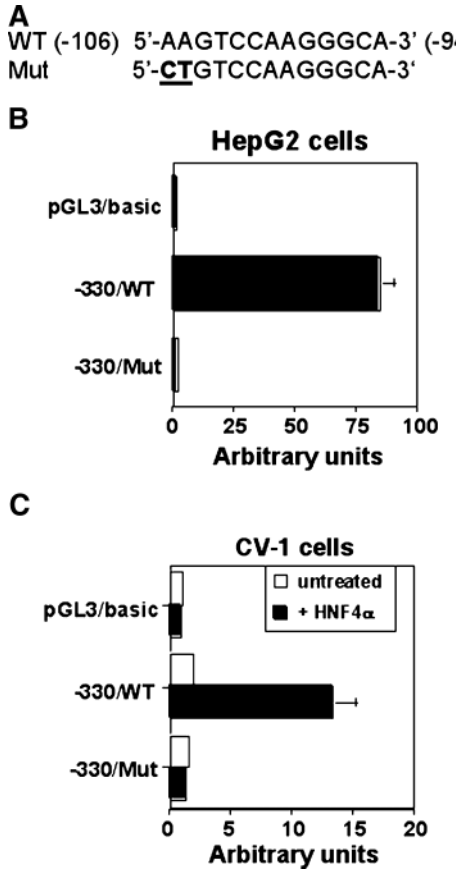

Fig. 7. Effects of mutations of the HNF4α binding site in the mouse *Cyp8b1* promoter. A: Scheme of the wild-type (WT) and mutated (Mut) HNF4α binding site of the mouse *Cyp8b1* promoter. Mutations in the HNF4α binding site are represented in boldface type and underlined. B, C: Plasmids were transfected into HepG2 (B) and CV-1 (C) cells, and the normalized activity ± SEM ($n = 4$) of each construct is presented as arbitrary units.

DISCUSSION

Cholesterol is hydroxylated by CYP7A1 and CYP27A1, the first enzymes in the classic and neutral BA biosynthesis pathways, respectively (12, 13). Human *Cyp7a1* has an HNF4α binding site in its promoter region (39, 40). However, the expression of CYP7A1 mRNA and protein was unchanged during the light cycle between HNF4α$^{\Delta L}$ and HNF4α$^{F/F}$ mice but higher during the dark cycle only in HNF4α$^{F/F}$ mice, indicating that HNF4α control of the *Cyp7a1* gene may only be significant during the dark cycle. It is possible that the influence of other transcription factors during the dark cycle is decreased, allowing HNF4α to predominate. Earlier studies have revealed that the expression of DBP, which is able to transactivate the *Cyp7a1* promoter, is correlated with CYP7A1 expression (37, 41). A relationship between DBP and HNF4α in the regulation of *Cyp7a1* has not been explored. Of interest, the expression of HNF4α was significantly increased in human liver biopsies from patients treated with cholestyramine in parallel with markedly increased expression of CYP7A1 (42), indicating that HNF4α may also regulate the expression of CYP7A1 in humans, as revealed by in vitro reporter gene studies (39, 40). It is not known whether the human gene is diurnally regulated. BA concentrations may also mask the influence of HNF4α on *Cyp7a1* expression. Because the enzyme activity of CYP7A1 and the mRNA encoding CYP27A1 are reduced and the BA excretion rate is also reduced, BA biosynthesis must also be lower in HNF4α$^{\Delta L}$ mice. In agreement with the CYP7A1 mRNA and protein expression data, the levels of 7α-hydroxycholesterol were reduced significantly in serum of HNF4α$^{\Delta L}$ mice compared with HNF4α$^{F/F}$ mice. A lower activity of the enzyme would be expected to result in less production of BAs and less feedback suppression of *Cyp7a1* through the FXR-SHP-liver receptor homologue-1 (LRH-1) pathway (43) and an increased expression of the gene. However, SHP mRNA levels are not significantly different between HNF4α$^{F/F}$ and HNF4α$^{\Delta L}$ mice (Table 2 and unpublished results). Clearly, the *Cyp7a1* gene is under complex regulation by FXR, SHP, LRH-1, liver X receptor, HNF4α (43), and DBP (41). Which of these factors predominates in the control of *Cyp7a1* will depend on the physiological situation.

Studies with the HNF4α$^{\Delta L}$ mice indicate that the *Cyp27a1* gene is directly regulated by HNF4α in vivo. This is in agreement with a recent report showing that HNF4α can bind to and transactivate the promoter region of the human *Cyp27a1* gene (44, 45). Thus, both mouse

Cyp27a1 and human *Cyp27a1* are direct targets for HNF4α. Interestingly, the levels of 27-hydroxycholesterol were significantly higher in HNF4α$^{\Delta L}$ mice than in HNF4α$^{F/F}$ mice. The circulating levels of this oxysterol are regulated by the relative activities of CYP27A1 and CYP7B1. Both *Cyp27a1* and *Cyp7b1* were downregulated in HNF4α$^{\Delta L}$ mice, but the downregulation of *Cyp7b1* was almost complete. Therefore, it seems likely that the increased levels of 27-hydroxycholesterol in HNF4α$^{\Delta L}$ mice reflect a markedly reduced metabolism of oxysterols. This finding was also observed in the *Cyp7b1*-null mice that have higher serum levels of both 25- and 27-hydroxycholesterol (46).

HNF4α binds to the promoter region of human *Cyp8b1* and activates transcription, as revealed by transactivation transcription assays (47). Other studies have suggested that BAs inhibit the expression of the rat *Cyp8b1* by inducing CPF/LRH-1 and inhibiting HNF4α expression (48). However, repression of *Cyp8b1* in HNF4α$^{\Delta L}$ mice might not be attributable to this negative feedback mechanism by BAs because CPF/LRH-1 is not induced in HNF4α$^{\Delta L}$ mice (8). The work described here indicates that HNF4α positively regulates the basal expression of *Cyp8b1* in vivo; thus, lower HNF4α that results from high BA levels could potentially cause a decrease in *Cyp8b1* transcription. It should also be noted that CYP8B1 is needed to synthesize CA, and *Cyp8b1*-null mice lack synthesis of CA and its metabolites (29). However, surprisingly, CA-derived metabolites (CA and DCA) in HNF4α$^{\Delta L}$ mice were not decreased compared with other BAs in the absence of CYP8B1 mRNA, and the concentration and/or total amount of CA in serum and gallbladder bile were increased along with other BAs. Furthermore, the enzyme activity of hepatic CYP8B1 was also markedly decreased, and no measurable levels of expression of CYP8B1 mRNA were detected in other tissues examined. We currently have no explanation for this discrepancy between CYP8B1 expression and CA levels.

The expression of CYP7B1 mRNA was almost extinguished in the HNF4α$^{\Delta L}$ mice. However, a functional HNF4α binding site could not be located in the *Cyp7b1* promoter region. Because expression of the human *Cyp7b1* gene is regulated by Sp1 (49), the mouse *Cyp7b1* gene might also be regulated by Sp1. Another mechanism involving Sp1 could also contribute to the loss of *Cyp7b1* gene expression in the HNF4α$^{\Delta L}$ mice. BA, found at high levels in HNF4α$^{\Delta L}$ mice, induces hepatic cytokine expression by activation of hepatic macrophage-like Kupffer cells (50). Tumor necrosis factor-α produced by these cells represses growth hormone receptor expression by inhibiting Sp1 and Sp3 binding to their corresponding sites in the promoter (51). Thus, hepatic production of tumor necrosis factor-α and other cytokines might be increased in HNF4α$^{\Delta L}$ mice, resulting in repression of the DNA binding activity of Sp1 family proteins to the *Cyp7b1* promoter. As discussed above, the expression of the major genes involved in BA biosynthesis is reduced in HNF4α$^{\Delta L}$ mice, including that encoding *Scpx*. This gene also does not contain a functional HNF4α site within proximity to its transcription start site, but it does contain GC-rich sequences that have potential Sp1 binding (data not shown). Thus, a mechanism similar to that described for the *Cyp7b1* gene may have a role in the loss of *Scpx* gene expression in HNF4α$^{\Delta L}$ mice. Finally, the presence of an HNF4α binding site at a remote distance from the *Cyp7b1* and *Scpx* promoters cannot be ruled out.

Because side chain β-oxidation of bile alcohols is catalyzed in peroxisomes, a deficiency in this pathway has been described as a secondary feature of various peroxisome disorders (52). The gene encoding SCPx also encodes SCP2, which contains the C-terminal sequence of SCPx (53), but the expression of SCP2 is unchanged (data not shown) because of the use of different promoters (32). *Scp2/Scpx*-null mice exhibit decreased catabolism of branched fatty acyl-CoA (54) and loss of side chain β-oxidation of bile alcohol at the thiolytic step (55), indicating that SCPx is indeed critical for side chain β-oxidation of bile alcohols. *Scp2/Scpx*-null mice also accumulate intermediate products of BA biosynthesis (55). These intermediate products might accumulate in HNF4α$^{\Delta L}$ mice as a result of the loss of SCPx expression, thus accounting for the additional unidentified peaks detected by LC-MS/MS in these mice.

After BA biosynthesis by hydroxylation of cholesterol and side chain β-oxidation, BAs are conjugated with taurine to produce bile salts in mice. The two main enzymes involved in BA conjugation are VLACSR and BA CoA: amino acid *N*-acyltransferase in mice. The expression of these genes was reduced in HNF4α$^{\Delta L}$ mice and dependent on HNF4α binding sites and HNF4α expression (11). Thus, HNF4α regulates all steps of BA biosynthesis, transport, and conjugation.

In conclusion, characterization of liver-specific HNF4α-null mice provided evidence for a critical role for hepatic HNF4α in the maintenance of BA homeostasis. Because other genes are also downregulated in the livers of HNF4α$^{\Delta L}$ mice in a mechanism that does not appear to involve HNF4α, further investigation of these genes might be useful to understand the regulation of the complete pathway of BA biosynthesis and transport and possibly to establish novel therapeutic targets for diseases resulting from altered BA homeostasis.

Liver samples from *Cyp8b1*-null and control mice and antibody against mouse CYP7A1 were kindly provided by Dr. David W. Russell (University of Texas Southwestern Medical Center, Dallas, TX). The authors thank Anita Lövgren-Sandblom and Maria Olin for their technical assistance. This work was partly supported by the Swedish Science Council and by the National Cancer Institute Intramural Research Program of the National Institutes of Health.

REFERENCES

1. Schrem, H., J. Klempnauer, and J. Borlak. 2002. Liver-enriched transcription factors in liver function and development. I. The hepatocyte nuclear factor network and liver-specific gene expression. *Pharmacol. Rev.* **54:** 129–158.

2. Sladek, F. M., and S. D. Seidel. 2002. Hepatocyte nuclear factor 4alpha. *In* Nuclear Receptors and Genetic Disease. T. P. Burris and E. McCabe, editors. Academic Press, San Diego, CA. 309–361.
3. Yamagata, K., H. Furuta, N. Oda, P. J. Kaisaki, S. Menzel, N. J. Cox, S. S. Fajans, S. Signorini, M. Stoffel, and G. I. Bell. 1996. Mutations in the hepatocyte nuclear factor-4alpha gene in maturity-onset diabetes of the young (MODY1). *Nature.* **384:** 458–460.
4. Reijnen, M. J., F. M. Sladek, R. M. Bertina, and P. H. Reitsma. 1992. Disruption of a binding site for hepatocyte nuclear factor 4 results in hemophilia B Leyden. *Proc. Natl. Acad. Sci. USA.* **89:** 6300–6303.
5. Gragnoli, C., T. Lindner, B. N. Cockburn, P. J. Kaisaki, F. Gragnoli, G. Marozzi, and G. I. Bell. 1997. Maturity-onset diabetes of the young due to a mutation in the hepatocyte nuclear factor-4 alpha binding site in the promoter of the hepatocyte nuclear factor-1 alpha gene. *Diabetes.* **46:** 1648–1651.
6. Yamagata, K., N. Oda, P. J. Kaisaki, S. Menzel, H. Furuta, M. Vaxillaire, L. Southam, R. D. Cox, G. M. Lathrop, V. V. Boriraj, et al. 1996. Mutations in the hepatocyte nuclear factor-1alpha gene in maturity-onset diabetes of the young (MODY3). *Nature.* **384:** 455–458.
7. Chen, W. S., K. Manova, D. C. Weinstein, S. A. Duncan, A. S. Plump, V. R. Prezioso, R. F. Bachvarova, and J. E. Darnell, Jr. 1994. Disruption of the HNF-4 gene, expressed in visceral endoderm, leads to cell death in embryonic ectoderm and impaired gastrulation of mouse embryos. *Genes Dev.* **8:** 2466–2477.
8. Hayhurst, G. P., Y. H. Lee, G. Lambert, J. M. Ward, and F. J. Gonzalez. 2001. Hepatocyte nuclear factor 4alpha (nuclear receptor 2A1) is essential for maintenance of hepatic gene expression and lipid homeostasis. *Mol. Cell. Biol.* **21:** 1393–1403.
9. Inoue, Y., G. P. Hayhurst, J. Inoue, M. Mori, and F. J. Gonzalez. 2002. Defective ureagenesis in mice carrying a liver-specific disruption of hepatocyte nuclear factor 4alpha (HNF4alpha). HNF4alpha regulates ornithine transcarbamylase in vivo. *J. Biol. Chem.* **277:** 25257–25265.
10. Bahar, J. R., and A. Stolz. 1999. Bile acid transport. *Gastroenterol. Clin. North Am.* **28:** 27–57.
11. Inoue, Y., A. M. Yu, J. Inoue, and F. J. Gonzalez. 2004. Hepatocyte nuclear factor 4alpha is a central regulator of bile acid conjugation. *J. Biol. Chem.* **279:** 2480–2489.
12. Bjorkhem, I., and G. Eggertsen. 2001. Genes involved in initial steps of bile acid synthesis. *Curr. Opin. Lipidol.* **12:** 97–103.
13. Chiang, J. Y. 2004. Regulation of bile acid synthesis: pathways, nuclear receptors, and mechanisms. *J. Hepatol.* **40:** 539–551.
14. Sinal, C. J., M. Tohkin, M. Miyata, J. M. Ward, G. Lambert, and F. J. Gonzalez. 2000. Targeted disruption of the nuclear receptor FXR/BAR impairs bile acid and lipid homeostasis. *Cell.* **102:** 731–744.
15. Peet, D. J., S. D. Turley, W. Ma, B. A. Janowski, J. M. Lobaccaro, R. E. Hammer, and D. J. Mangelsdorf. 1998. Cholesterol and bile acid metabolism are impaired in mice lacking the nuclear oxysterol receptor LXR alpha. *Cell.* **93:** 693–704.
16. del Castillo-Olivares, A., and G. Gil. 2000. Alpha 1-fetoprotein transcription factor is required for the expression of sterol 12alpha -hydroxylase, the specific enzyme for cholic acid synthesis. Potential role in the bile acid-mediated regulation of gene transcription. *J. Biol. Chem.* **275:** 17793–17799.
17. Staudinger, J. L., B. Goodwin, S. A. Jones, D. Hawkins-Brown, K. I. MacKenzie, A. LaTour, Y. Liu, C. D. Klaassen, K. K. Brown, J. Reinhard, et al. 2001. The nuclear receptor PXR is a lithocholic acid sensor that protects against liver toxicity. *Proc. Natl. Acad. Sci. USA.* **98:** 3369–3374.
18. Xie, W., A. Radominska-Pandya, Y. Shi, C. M. Simon, M. C. Nelson, E. S. Ong, D. J. Waxman, and R. M. Evans. 2001. An essential role for nuclear receptors SXR/PXR in detoxification of cholestatic bile acids. *Proc. Natl. Acad. Sci. USA.* **98:** 3375–3380.
19. Hunt, M. C., Y. Z. Yang, G. Eggertsen, C. M. Carneheim, M. Gafvels, C. Einarsson, and S. E. Alexson. 2000. The peroxisome proliferator-activated receptor alpha (PPARalpha) regulates bile acid biosynthesis. *J. Biol. Chem.* **275:** 28947–28953.
20. Kerr, T. A., S. Saeki, M. Schneider, K. Schaefer, S. Berdy, T. Redder, B. Shan, D. W. Russell, and M. Schwarz. 2002. Loss of nuclear receptor SHP impairs but does not eliminate negative feedback regulation of bile acid synthesis. *Dev. Cell.* **2:** 713–720.
21. Wang, L., Y. K. Lee, D. Bundman, Y. Han, S. Thevananther, C. S. Kim, S. S. Chua, P. Wei, R. A. Heyman, M. Karin, et al. 2002. Redundant pathways for negative feedback regulation of bile acid production. *Dev. Cell.* **2:** 721–731.
22. Shih, D. Q., M. Bussen, E. Sehayek, M. Ananthanarayanan, B. L. Shneider, F. J. Suchy, S. Shefer, J. S. Bollileni, F. J. Gonzalez, J. L. Breslow, et al. 2001. Hepatocyte nuclear factor-1alpha is an essential regulator of bile acid and plasma cholesterol metabolism. *Nat. Genet.* **27:** 375–382.
23. Coffinier, C., L. Gresh, L. Fiette, F. Tronche, G. Schutz, C. Babinet, M. Pontoglio, M. Yaniv, and J. Barra. 2002. Bile system morphogenesis defects and liver dysfunction upon targeted deletion of HNF1beta. *Development.* **129:** 1829–1838.
24. Yu, C., F. Wang, M. Kan, C. Jin, R. B. Jones, M. Weinstein, C. X. Deng, and W. L. McKeehan. 2000. Elevated cholesterol metabolism and bile acid synthesis in mice lacking membrane tyrosine kinase receptor FGFR4. *J. Biol. Chem.* **275:** 15482–15489.
25. Yim, S. H., J. M. Ward, Y. Dragan, A. Yamada, P. C. Scacheri, S. Kimura, and F. J. Gonzalez. 2003. Microarray analysis using amplified mRNA from laser capture microdissection of microscopic hepatocellular precancerous lesions and frozen hepatocellular carcinomas reveals unique and consistent gene expression profiles. *Toxicol. Pathol.* **31:** 295–303.
26. Dzeletovic, S., O. Breuer, E. Lund, and U. Diczfalusy. 1995. Determination of cholesterol oxidation products in human plasma by isotope dilution-mass spectrometry. *Anal. Biochem.* **225:** 73–80.
27. Rosen, H., A. Reshef, N. Maeda, A. Lippoldt, S. Shpizen, L. Triger, G. Eggertsen, I. Bjorkhem, and E. Leitersdorf. 1998. Markedly reduced bile acid synthesis but maintained levels of cholesterol and vitamin D metabolites in mice with disrupted sterol 27-hydroxylase gene. *J. Biol. Chem.* **273:** 14805–14812.
28. Vlahcevic, Z. R., G. Eggertsen, I. Bjorkhem, P. B. Hylemon, K. Redford, and W. M. Pandak. 2000. Regulation of sterol 12alpha-hydroxylase and cholic acid biosynthesis in the rat. *Gastroenterology.* **118:** 599–607.
29. Li-Hawkins, J., M. Gafvels, M. Olin, E. G. Lund, U. Andersson, G. Schuster, I. Bjorkhem, D. W. Russell, and G. Eggertsen. 2002. Cholic acid mediates negative feedback regulation of bile acid synthesis in mice. *J. Clin. Invest.* **110:** 1191–1200.
30. Gafvels, M., M. Olin, B. P. Chowdhary, T. Raudsepp, U. Andersson, B. Persson, M. Jansson, I. Bjorkhem, and G. Eggertsen. 1999. Structure and chromosomal assignment of the sterol 12alpha-hydroxylase gene (CYP8B1) in human and mouse: eukaryotic cytochrome P-450 gene devoid of introns. *Genomics.* **56:** 184–196.
31. Bjorkhem, I., E. Reihner, B. Angelin, S. Ewerth, J. E. Akerlund, and K. Einarsson. 1987. On the possible use of the serum level of 7 alpha-hydroxycholesterol as a marker for increased activity of the cholesterol 7 alpha-hydroxylase in humans. *J. Lipid Res.* **28:** 889–894.
32. Toll, A., K. Wikvall, E. Sudjana-Sugiaman, K. H. Kondo, and I. Bjorkhem. 1994. 7 alpha hydroxylation of 25-hydroxycholesterol in liver microsomes. Evidence that the enzyme involved is different from cholesterol 7 alpha-hydroxylase. *Eur. J. Biochem.* **224:** 309–316.
33. Schwarz, M., E. G. Lund, R. Lathe, I. Bjorkhem, and D. W. Russell. 1997. Identification and characterization of a mouse oxysterol 7alpha-hydroxylase cDNA. *J. Biol. Chem.* **272:** 23995–24001.
34. Li-Hawkins, J., E. G. Lund, A. D. Bronson, and D. W. Russell. 2000. Expression cloning of an oxysterol 7alpha-hydroxylase selective for 24-hydroxycholesterol. *J. Biol. Chem.* **275:** 16543–16549.
35. Ohba, T., J. A. Holt, J. T. Billheimer, and J. F. Strauss 3rd. 1995. Human sterol carrier protein x/sterol carrier protein 2 gene has two promoters. *Biochemistry.* **34:** 10660–10668.
36. Noshiro, M., M. Nishimoto, and K. Okuda. 1990. Rat liver cholesterol 7 alpha-hydroxylase. Pretranslational regulation for circadian rhythm. *J. Biol. Chem.* **265:** 10036–10041.
37. Yamada, M., J. Nagatomo, Y. Setoguchi, N. Kuroki, S. Higashi, and T. Setoguchi. 2000. Circadian rhythms of sterol 12alpha-hydroxylase, cholesterol 7alpha-hydroxylase and DBP involved in rat cholesterol catabolism. *Biol. Chem.* **381:** 1149–1153.
38. Ishida, H., Y. Kuruta, O. Gotoh, C. Yamashita, Y. Yoshida, and M. Noshiro. 1999. Structure, evolution, and liver-specific expression of sterol 12alpha-hydroxylase P450 (CYP8B). *J. Biochem. (Tokyo).* **126:** 19–25.
39. Cooper, A. D., J. Chen, M. J. Botelho-Yetkinler, Y. Cao, T. Taniguchi, and B. Levy-Wilson. 1997. Characterization of hepatic-specific regulatory elements in the promoter region of the human cholesterol 7alpha-hydroxylase gene. *J. Biol. Chem.* **272:** 3444–3452.
40. Crestani, M., A. Sadeghpour, D. Stroup, G. Galli, and J. Y. Chiang. 1998. Transcriptional activation of the cholesterol 7alpha-hydroxylase gene (CYP7A) by nuclear hormone receptors. *J. Lipid Res.* **39:** 2192–2200.
41. Lee, Y. H., J. A. Alberta, D. J. Waxman, and F. J. Gonzalez. 1994. Multiple, functional DBP sites on the promoter of the cholesterol

7 alpha-hydroxylase P450 gene, CYP7. Proposed role in diurnal regulation of liver gene expression. *J. Biol. Chem.* **269:** 14681–14689.
42. Abrahamsson, A., U. Gustafsson, E. Ellis, L. M. Nilsson, S. Sahlin, I. Bjorkhem, and C. Einarsson. 2005. Feedback regulation of bile acid synthesis in human liver: importance of HNF-4alpha for regulation of CYP7A1. *Biochem. Biophys. Res. Commun.* **330:** 395–399.
43. Davis, R. A., J. H. Miyake, T. Y. Hui, and N. J. Spann. 2002. Regulation of cholesterol-7alpha-hydroxylase: BAREly missing a SHP. *J. Lipid Res.* **43:** 533–543.
44. Garuti, R., M. A. Croce, L. Piccinini, R. Tiozzo, S. Bertolini, and S. Calandra. 2002. Functional analysis of the promoter of human sterol 27-hydroxylase gene in HepG2 cells. *Gene.* **283:** 133–143.
45. Chen, W., and J. Y. Chiang. 2003. Regulation of human sterol 27-hydroxylase gene (CYP27A1) by bile acids and hepatocyte nuclear factor 4alpha (HNF4alpha). *Gene.* **313:** 71–82.
46. Li-Hawkins, J., E. G. Lund, S. D. Turley, and D. W. Russell. 2000. Disruption of the oxysterol 7alpha-hydroxylase gene in mice. *J. Biol. Chem.* **275:** 16536–16542.
47. Zhang, M., and J. Y. Chiang. 2001. Transcriptional regulation of the human sterol 12alpha-hydroxylase gene (CYP8B1): roles of hepatocyte nuclear factor 4alpha in mediating bile acid repression. *J. Biol. Chem.* **276:** 41690–41699.
48. Yang, Y., M. Zhang, G. Eggertsen, and J. Y. Chiang. 2002. On the mechanism of bile acid inhibition of rat sterol 12alpha-hydroxylase gene (CYP8B1) transcription: roles of alpha-fetoprotein transcription factor and hepatocyte nuclear factor 4alpha. *Biochim. Biophys. Acta.* **1583:** 63–73.
49. Wu, Z., and J. Y. Chiang. 2001. Transcriptional regulation of human oxysterol 7 alpha-hydroxylase gene (CYP7B1) by Sp1. *Gene.* **272:** 191–197.
50. Miyake, J. H., S. L. Wang, and R. A. Davis. 2000. Bile acid induction of cytokine expression by macrophages correlates with repression of hepatic cholesterol 7alpha-hydroxylase. *J. Biol. Chem.* **275:** 21805–21808.
51. Denson, L. A., R. K. Menon, A. Shaufl, H. S. Bajwa, C. R. Williams, and S. J. Karpen. 2001. TNF-alpha downregulates murine hepatic growth hormone receptor expression by inhibiting Sp1 and Sp3 binding. *J. Clin. Invest.* **107:** 1451–1458.
52. Balistreri, W. F. 1999. Inborn errors of bile acid biosynthesis and transport. Novel forms of metabolic liver disease. *Gastroenterol. Clin. North Am.* **28:** 145–172.
53. Ohba, T., H. Rennert, S. M. Pfeifer, Z. He, R. Yamamoto, J. A. Holt, J. T. Billheimer, and J. F. Strauss 3rd. 1994. The structure of the human sterol carrier protein X/sterol carrier protein 2 gene (SCP2). *Genomics.* **24:** 370–374.
54. Seedorf, U., M. Raabe, P. Ellinghaus, F. Kannenberg, M. Fobker, T. Engel, S. Denis, F. Wouters, K. W. Wirtz, R. J. Wanders, et al. 1998. Defective peroxisomal catabolism of branched fatty acyl coenzyme A in mice lacking the sterol carrier protein-2/sterol carrier protein-x gene function. *Genes Dev.* **12:** 1189–1201.
55. Kannenberg, F., P. Ellinghaus, G. Assmann, and U. Seedorf. 1999. Aberrant oxidation of the cholesterol side chain in bile acid synthesis of sterol carrier protein-2/sterol carrier protein-x knockout mice. *J. Biol. Chem.* **274:** 35455–35460.